Developing pressure sensors from impregnated textile sandwiched in inkjet-printed electrodes

Saleem Khan[1,*] , Shawkat Ali[1], Arshad Khan[1], and Amine Bermak[1]

[1] *Division of Information and Computing Technology, College of Science and Engineering, Hamad Bin Khalifa University, Ar-Rayyan, Qatar*

ABSTRACT

This work presents an interesting fabrication route toward development of pressure sensing patch by utilizing electrically conductive cotton fabric sandwiched between two parallel electrodes. An all-printing strategy is adopted to simplify the manufacturing and minimize the overall cost. A conductive nanocomposite solution is developed by mixing carbon-based paste and an organic conductor PEDOT-PSS (poly(3,4-ethylenedioxythiophene). Several mixing ratios were investigated to analyze the optimal coating parameters and resulting percolation thresholds. A nanofibrous and stretchable cotton fabric is selected for impregnation with the nanocomposite solution, which is used as the pressure sensing layer. The metallic plates and interconnect lines are developed by inkjet printing Ag nanoparticles-based solution on a PET (polyethylene terephthalate) substrate. The thermally sensitive resin on one side of PET substrate enables sandwiching the impregnated fabric through lamination. A 3×3 sensing array is developed with each sensing cell having 5×5 mm^2 effective area. The piezoresistance is determined by exploiting the change in bulk resistance of the electrically conducting fabric caused by the physical deformations at microscale in the conductive threads partly due to percolation mechanism. The produced sensors are tested and are able to record resistance variation for as small as 1 gm weight. The results show that this type of sensors can successfully be applied for a wide variety of pressure mapping and force monitoring system requiring deployment on large areas.

1 Introduction

Printing electronic devices and sensors over wide area and different polymeric substrates have emerged significantly in recent years [1–3]. Additive manufacturing for thin film deposition as well high-resolution patterning have revolutionized the manufacturing of electronic components. The attractive features such as less processing steps, drop-on-demand deposition of diverse functional nanomaterials, and development of multilayers structures on unconventional substrates make printing a unique

Springer

cost-effective manufacturing technology [4–6]. The rapidly growing interest in printing technologies especially for the development of large area sensors and electronics is evidenced by the publication of large number of research articles [1, 5, 7, 8]. The use of unconventional polymeric substrates with unique properties such as flexibility, foldability, lightweight, portability and conformal integration on non-planar surface make them ideal for development of large-scale devices [9–12]. Therefore, printing technologies are enabling a new era of macroelectronics, where the geometric sizes of the electronic components are millimeters wide as against the conventional dimensions of microelectronic devices. This approach has already produced exciting results and numerous proof of concept devices are showcased by many research groups [13–17]. Diversity of applications ranges from industry, environmental and especially biomedical entities.

Among the list of proposed active and passive devices developed thus far, research on large area pressure sensors has gained significant interest due to its multitude functions [16, 18–20]. Covering large area and soft integration to both planar and non-planar surfaces make these pressure sensors ideal for applications such as prosthetic devices, electronic/robotic skin, and smart mats for hospital beds [17, 19, 21]. With the fast emergence of IoT (internet of things) and smart city strategies, these large area sensors have found new venues of applications. For instance, waste collection in an efficient way is an integral part of a smart city development, where all the collection sites/containers are equipped with sensory patches to monitor their fill levels or their readiness to be emptied [22]. In this perspective, cost-effective and large area pressure sensors play significant role in level monitoring of the waste collection bins.

Diverse transduction mechanisms are in practice for measuring the pressure/force measurement [23]. Among these, piezoresistance films made of nanocomposite films offer more advantages due to the low cost of conducting nanofillers, simple, material-efficient deposition low-cost processing technologies [24–27]. A range of piezoresistance-based sensors are being developed utilizing different materials and mechanisms that include resistance changes in strain gauges, change in mobility of solid-state semiconductor devices [28–30]. The new approaches developed recently by mixing conductive nanofillers in a polymeric matrix to exploit the percolation mechanism upon force application have gained particular attention [31–33]. However, retaining fixed mixing ratios of the nanofillers in polymer matrix, uniform mixing and finally printing in a patterned fashion is challenging to reproduce the sensors on large scale at similar sensing ranges. The recent developments in using conducting yarns have gained momentum [34]. This technique employs the use of normal yarns, which are dipped to impregnate the thread with electrically conducting materials [35, 36]. This approach although allows the use of these threads for pressure sensing and metallic interconnects; however, pattered orientation of the threads is a serious challenge. The effective sensing areas relies on width and length of the conducting yarn and covering large area with these conducting yarns requires extra effort as most of the development is done manually. Besides, the rapid and reproducible manufacturing of sensors covering larger area is hard to produce. A new approach by patterning sandwiching an electrically conducting cotton fabric within two printed metallic electrodes is explored.

The cotton fabric is impregnated with a mixture of carbon and PEDOT-PSS according to the designated array configuration. A 3×3 array of sensors is designed to cover a larger area of about 100 mm². To make the manufacturing process easier and cost-effective, an all-printing approach is adopted. The Ag-based electrodes and interconnections are patterned using drop-on-demand inkjet printing and the sensing blocks are patterned using screen-printing technology. This paper is focused on the manufacturing with a particular focus on deterministic placement of dissimilar materials and adhesion of these to the substrates, conformal attachability of the three substrates. Focus on reducing the processing steps and assembly of the sensor patches at minimal control parameters are explored. Response of the sensors is evaluated at different compressive forces.

2 Working principle

Working mechanism of the conducting fabric is similar to a strain sensor. Each conducting yarn is comprised of micron scale fiber and are loosely threaded. When an external force is applied, a compression is caused in these micron scale threaded

fibers that lead to the change in bulk resistance. Figure 1 shows the fibrous yarn in normal condition. The loosen conductive threads (with an average spacing about 10 μm) work in similar fashion to the percolation, where electric conductive path and networks are established by applying a compressive force on a piezoresistive structure [25, 27]. The interconnections and conducting network made by the mesh as well as by the threads within a single yarn produce a base electrical resistance upon impregnation. However, these voids still remain after coating with the conductive nanocomposite and are exploited to determine the external applied forces. The base resistance is reached back once the applied force is removed and the conductive threads are relaxed to the normal position. The strain-related properties of this conducting fabric can be exploited both for longitudinal and transversal applied forces. This research is focused on the detection and measurement of transversal applied forces, where this conducting fabric is sandwiched within two parallel printed metallic plates.

3 Materials and sensor schematics

3.1 Nanocomposite paste development

The nanocomposite used for development of the sensor patch is synthesized by mixing carbon-based paste (purchased from Sigma-Aldrich (Product No. 699624)) and PEDOT-PSS polystyrene sulfonate) (Sigma-Aldrich). The mixing ratio of 2 wt% is
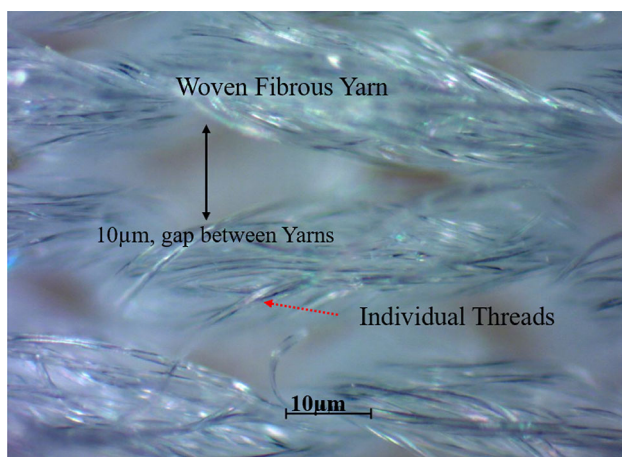

Fig. 1 Optical micrograph of a stretchable fabric and view of the individual fibrous threads

optimized for carbon and PEDOT-PSS, respectively, after observing the printability, uniformity and finally the sensing response. PEDOT-PSS is an electrically conducting material and commonly used as electrode for many organic electronic devices and sensing applications. Mixing carbon and PEDOT-PSS produce exciting electrical and physical properties, especially for the percolation-based sensing applications. The change in electrical resistance against external force is exploited to determine the applied force. Percolation mechanism is responsible for such monitoring as the compressible conducting interconnecting paths contribute to the resistance change [31]. To retain the physical, mechanical, and electrical properties, a low mixing ratios and percolation threshold are desired. The lower mixing threshold also contributes to the uniform dispersion of nano-filler components that significantly influences the sensor performances.

Despite the fact that these polymers-based nanocomposites produce non-linear responses, they have considerable hysteresis as well as drifts occurring due to temperature, yet they are good alternatives for low-cost strain sensing applications deployed on larger areas. To exploit the compressibility properties of the fabric, the conductive nanocomposite material is applied on both the sides to make conductive threads within the cotton fabric. The nanocomposite is synthesized by mixing carbon-based paste (purchased from Sigma-Aldrich) and PEDOT-PSS (purchased from Sigma-Aldrich). Various mixing ratios were tried and the one selected (i.e., 2 wt%) is kept at ranges that are more suitable for the screen-printing processes. The PEDOT-PSS is used to enhance the conductivity as well as the absorption within the cotton fabric. After the mechanical stirring, the solution is kept in ultrasonic bath at 40 kHz for 1 hour. The nanocomposite paste is applied immediately on the cotton fabric using stencil printing.

3.2 Schematic of the sensor module

A parallel plate configuration is intended, where the cotton fabric is sandwiched between two PET sheets with printed electrodes on the thermally sensitive sides. Figure 2 shows schematic of the proposed model following a 3×3 arrayed design. Sensor patch is designed such that all the sensing units are distant apart and covering much larger area as possible. The active area of an individual sensor is kept at 5×5 mm^2
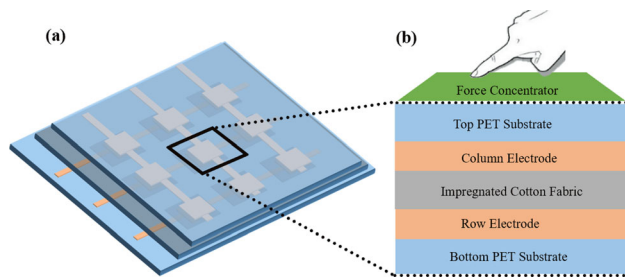
Fig. 2 Schematic diagram of sensor module and cross-sectional view of the proposed printed layers

and the distance between the neighboring sensors is maintained at 25 mm. The impregnated area of fabric, i.e., 6×6 mm^2, is enlarged in order to fully cover the electrodes as well as avoid short-circuiting of the interconnecting lines. The deterministic placement and conformal integration of these dissimilar substrates is highly desired. Figure 2a shows the top view of the sensing structure, whereas cross-section of the sensor is shown in Fig. 2b. To converge the applied external force at the sensing area, force concentrator structures are developed by casting glue at corresponding positions on the top surface. The whole sensing module is designed such that all the printed materials and structures are encapsulated by default except the contacting pads.

3.3 Substrates

The mechanical flexibility, bendability, stretchability, and conformal integration of polymeric substrates are the key enablers for fabrication of large area light weight sensing systems. The multifunctional polymeric substrates provide a strong base upon which the various printed sensors are reliably developed. Substrates play an important role in design of experiments and selection of suitable materials for fabrication of multi-layered sensing devices. All the materials involved in the development including the substrates are required to have thermal, physical, and mechanical properties in close ranges to enhance the compliant integration with each other as well as with non-planar surfaces. In this research, two different substrates are selected. A special type of polyethylene terephthalate PET (purchased from Sigma-Aldrich) substrate is used. One side of the PET substrate is pre-coated with a thermally sensitive resin layer. This resin layer is required for the thermal lamination step of the fabrication process, where the pressure sensing

fabric is sandwiched between such two sheets. The top and bottom electrodes are developed on two different PET sheets. Secondly for impregnation purposes, a cotton fabric (purchased from TekniZorb) is used for developing the pressure sensing layer. The absorption capability of the cotton fabric is exploited to impregnate it with pressure sensing nanocomposite layer. To make the parallel plate structure, the thermal lamination of PET substrates on both sides of the cotton fabric is used to make the sandwich structure. No special treatment of the substrates is required that also makes the manufacturing process simpler and cost-effective.

4 Printing experiments

4.1 Inkjet printing of top and bottom electrodes

Inkjet printing is a robust additive manufacturing technique used for patterning of solution-based functional materials. Rheological properties of the solutions are tuned and adjusted according to the desired requirements of inkjet printing systems. The piezoelectric actuation-based inkjet printing is more popular as it can be used to process a wide variety of organic and inorganic materials [5, 10, 15]. The controlled ejection and manipulation of the droplet volume as well as the deterministic placement of patterns at targeted locations (schematic in Fig. 3a), make this process distinguished from other additive manufacturing techniques. Ag nanoparticles-based ink at pre-adjusted properties for inkjet printing is used to pattern the metallic electrodes. The substrates are kept at 40 °C, whereas the nozzle printhead is heated at 35 °C, as an optimized parameter for uniform jetting. The electrodes are printed on the side which is coated with thermally sensitive resin. The resin surface is not ideally smooth as desired for the printable structures, therefore multiple printing cycles are executed to guarantee the electrical conduction as well as the strong physical adherence of printed structures to the target substrate. The conducting structures consisted of metallic plates, interconnect lines and contacting pads. An array of 3×3 sensing cells (as shown in Fig. 3b) is printed using Dimatix 2850 inkjet printing system. All the printing parameters are adjusted based on the experimental investigations and the resulting behavior of the ink

Fig. 3 **a** Schematics of drop-on-demand inkjet printing. **b** Printed results of Ag electrodes on thermally sensitive resin side of PET substrate ((i). array of sensors, (ii) optical image of a single electrode, (iii) SEM image of the printed Ag)

(a)

(b)
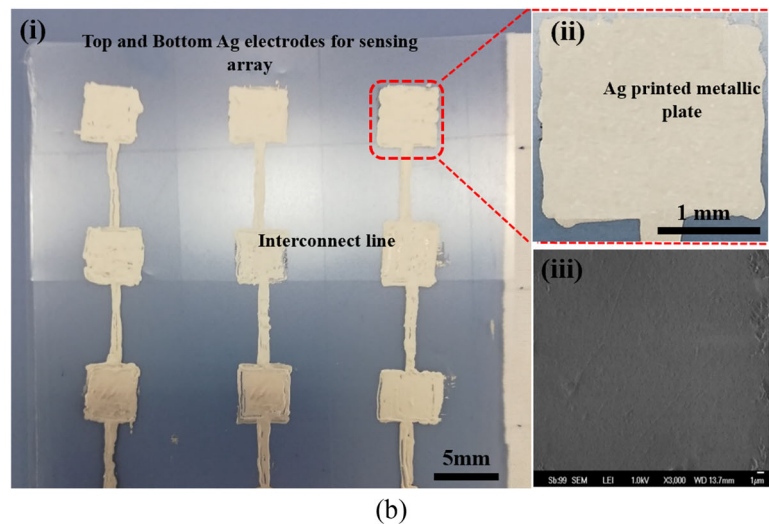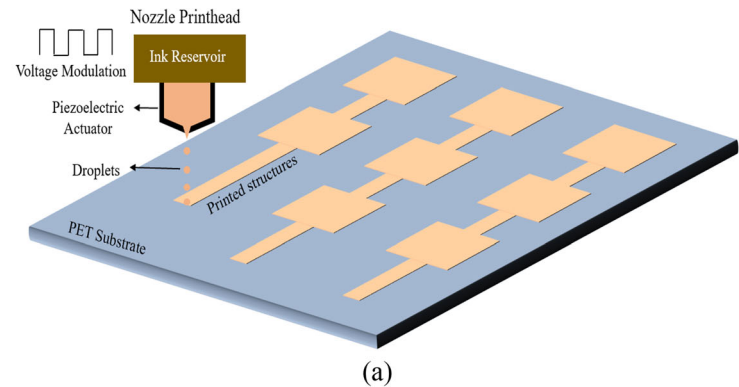
with the target substrate. Few of the critical parameters that play significant role in producing better printing results include jetting waveform, frequency, impacting velocity, substrate treatment conditions, standoff distance, and drop-to-drop spacing, etc. The jetting frequency at 2 kHz, velocity 7 mm/sec, substrate temperatures 45 °C, standoff distance 0.5 mm, and inter-drops spacing of 25μm were observed to be the critical parameters that produced promising printing results. All these parameters were adjusted to produce the best possible results. Total of five printing cycles were executed to create the desired structures. The substrate is kept at 80 °C overnight in an oven for thermal treatment. Figure 3b shows printed results after curing. Similar structure is printed for the top electrodes on the same type of substrate using the optimized inkjet printing parameters.

4.2 Printing nanocomposite on stretchable fabric

A stretchable fabric is selected for developing the force sensing layer. The fabric is placed on a planar support with pre-stretched condition, to allow the maximum impregnation and complete absorption of the nanocomposite material on both the sides. This also allows for the nanocomposite material to penetrate easily within the fabric mesh by making individual thread conducting. A similar approach has been reported previously, by impregnating stretchable fabric with Silver paste [36]. The solution is casted and patterned according to the geometric parameters of the top and bottom electrodes. Figure 4b shows schematic representation of the nanocomposite coating on fabric. The shadow mask is prepared by Laser cutting a plastic sheet. The masking sheet is selected based on the thickness (i.e., 150 μm), it allows sufficient volume of nanocomposite to contain. Besides casting, the containment well

(a)

(b)
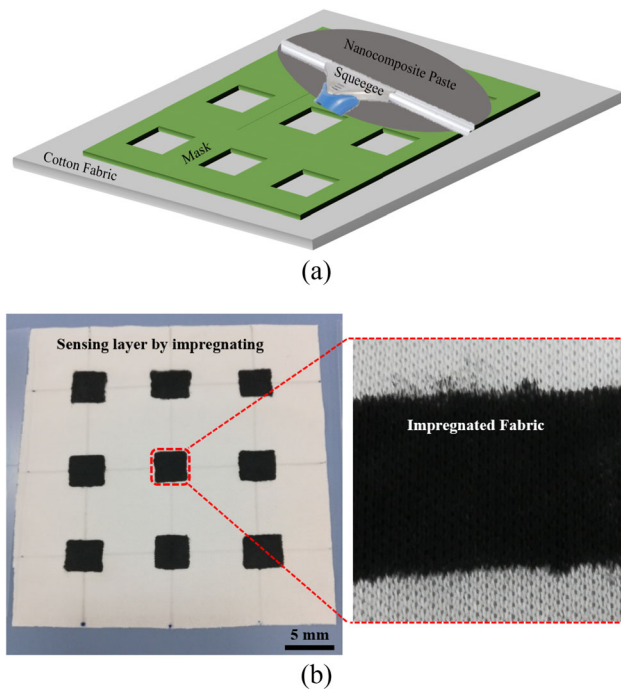
Fig. 4 **a** Schematic of screen-printing setup, **b** sensing array by nanocomposite printing

of the shadow mask is also filled with extra nanocomposite material to allow maximum impregnation of the fabric. The impregnated area is kept at 6×6 mm^2, an enlarged area than the electrodes plates. This is designed to avoid any short-circuiting of the top and bottom electrodes that could occur in case of minor misalignments during thermal lamination. After coating, the fabric is released from the pre-stretched condition and the nanocomposite material is allowed to dry overnight at 60 °C in the oven. Figure 4b shows results of the solidified nanocomposite structures.

4.3 Assembly through thermal lamination

Thermal lamination is process where multiple layers or sheets of different materials are combined using controlled hot pressing. Sophisticated machines are used such as desktop laminator for a smaller number of sheets, whereas multilayer-press is practiced for large-scale processing. In these experiments, the commonly used desktop thermal laminator is used to make the sandwiched structure. The fabric is placed between the two PET substrates with good alignment of the sensing area between top and bottom electrodes. Temperature is adjusted at about 250 °C (measured with a thermocouple) and at normal

pressure were sufficient to melt the resin and attach to the fabric instantaneously. Pads of the printed electrodes were left bar for the wire attachment and readout. Figure 5a–c shows images of the individual printed structures and final assembled sensing array, respectively. The wires are attached to the pads using silver conducting epoxy.
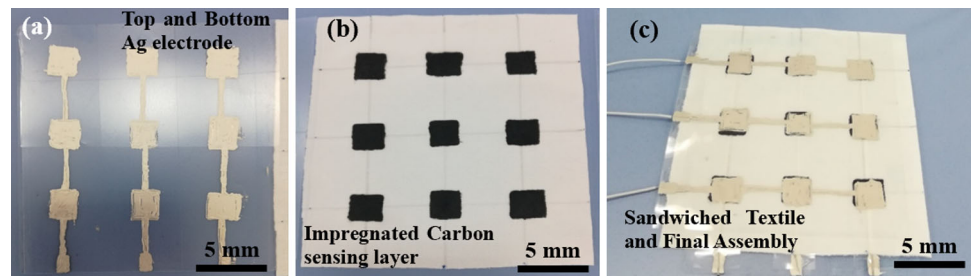
5 Results and discussion

The various physical and electrical properties of the inkjet-printed metallic structures as well as the sensing layers were determined using standard characterization techniques. Thickness of the printed conducting patterns is of prime importance to guarantee reliable metal plates as well as interconnections. Profilometer is used to evaluate the thickness of printed patterns. Similarly, adhesion-loss test, print efficiency and sheet resistance are also determined. Impregnation of the fabric with conductive nanocomposite based on the deposition quantity to enable the absorbance through the fabric onto the back side is critical for sensor performance. All these properties were evaluated in ambient environment and described in more detail in the following sections.

5.1 Sheet resistance of conducting patterns

Sheet resistance of the conducting patterns is measured both in planar as well as in bent mode to check for the conductivity variations. The standard technique of four-point probe measurement is used to determine the sheet resistance. A high impedance Keithley 7410 sourcemeter was used for current and voltage measurements across the printed structures. The four points for probing on the printed lines was selected such that almost all the longitudinal area would be covered. Therefore, each of the probe is attached to the metallic plates connected linearly in a single row. Current is applied at the external two probes, while the internal two probes are used to determine the voltage drop. The reference values provided by the Ag paste supplier is about 12 Ω/sq. for an approximate layer thickness of about 25 μm. In this case, the sheet resistance for a layer thickness of about 6 μm achieved is approximately 15.2 Ω/sq., which is not a major deviation from the expected resistivity. The same type of printed structures were

Fig. 5 **a** Screen-printed MWCNT/PDMS on PET substrate **b** final assembled sensor cell with force concentrator structures


5.2 Microscopic analysis

Quality of the impregnation of stretchable fabric with nanocomposite paste as well as the printed silver contacts were analyzed using optical microscope. Figure 7 shows image of the impregnated threads after complete drying of the solvents added in the nanocomposite composition. It is evident that each of the thread is completely coated both on the interior and external micron scale fibers making the thread. The porous structure is observed (as shown in the Fig. 6) in the fabric that indicates the complete evaporation of the surfactants added for uniform

tested under bending conditions for further exploration using the similar testing configuration. The substrate is bent at a radius of about 20 mm to confirm any significant deviation in the conductivity when changing the orientation of the substrates. However, no considerable change in the voltage drop at the central probes is observed by applying the same amount of current at the external probes. This negligible change might be contributed by the relatively thicker film deposition as well as the wider area printing of the conductive patterns.

mixing of the nanocomposite material. The inter-fiber spacing as well as the gaps between neighboring threads provide an opportunity to exploit such structures for percolation mechanism. Compressibility of the individual fibers itself and shrinkage of the fibers as against the external compressive force leads to change in the electrical conductivity of the stretchable fabric. This porous structure also provides a strong support by sustaining high pressures as well as angular deflection due to the least residual stresses. Figure 7 shows surface morphology of the impregnated fabric observed through 3-D Nanoprofiler. It is evident both from the top and 3-D view that, the nanocomposite layer is completely impregnated within the fibers and the spacings between each thread further confirms the inter-threads spacing ideal for the percolation mechanism.

Mechanical profilometer is used to determine the thickness of the printed silver patterns. Conventionally screen-printing is used for thick film deposition, which is more suitable for such type of applications. As a considerable elevation on a micron scale is preferred compared to the substrate surface, it will provide an intimate contact between the sensing layer and the conducting Ag plates. Five passages of

Fig. 6 **a**, **b** Optical inspection of the cured nanocomposite-coated fabric and a close look-up of the corresponding porosity. (c) SEM of the impregnated cotton fabric with nanocomposite material
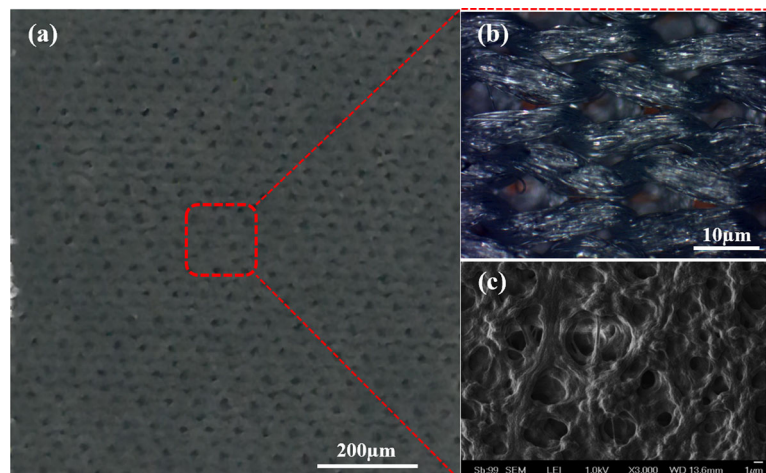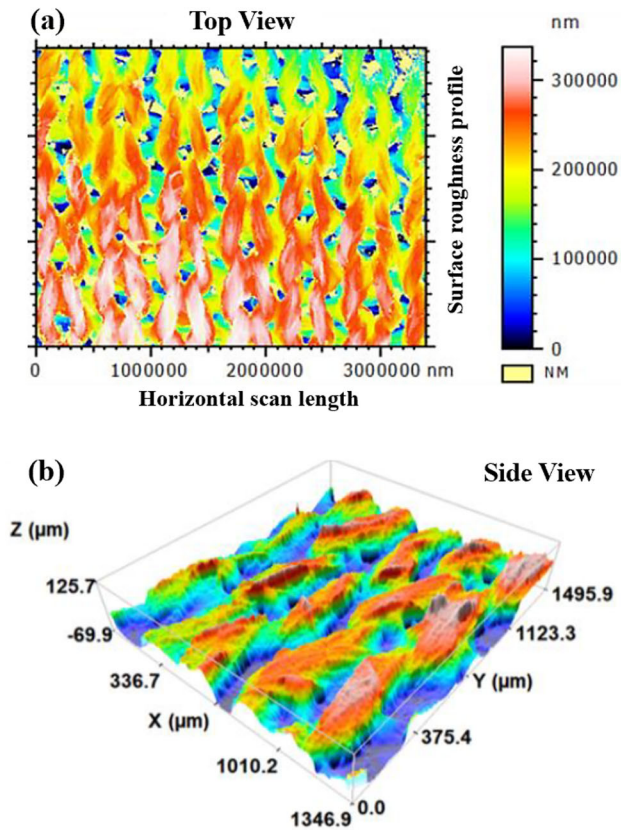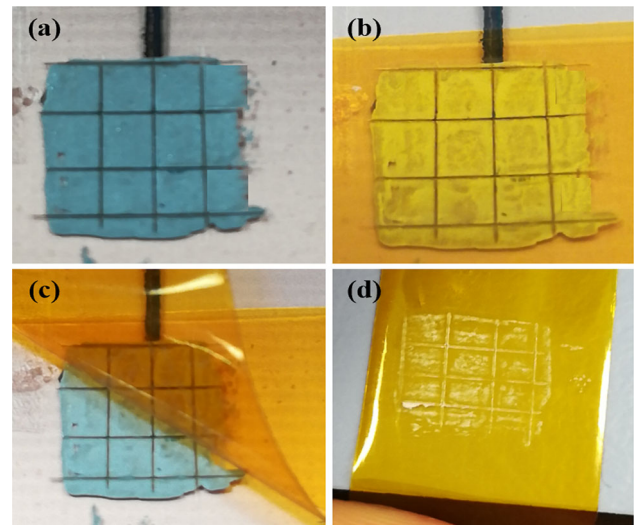
Fig. 7 **a** Surface morphology and, **b** 3-D view of the impregnated fabric observed through 3-D Nanoprofiler

Fig. 8 Adhesion-loss test when, **a** no tape applied, **b** tape is applied, **c** removing, **d** complete removal and observation of the detachment

the inkjet printing achieved thickness of about 1.5 μm after complete sintering of the printed structures. Similarly, the adhesion-loss tests were conducted both on the impregnated fabric as well as on the Ag-printed structures. As a result of complete impregnation, the nanocomposite becomes integral part of the fabric and by applying a blue scotch tape on the surface, no residual is observed, showing a complete absorption of the ink within the fabric threads. The standard cut and tape test was performed to see the detachment of Ag patterns from the thermally sensitive PET substrate. Figure 8a–d shows images of the printed Ag structures before and after adhesion-loss test. A strong attachability of the Ag patterns to the target substrate is evidenced after performing the tape test 5 times on a single sample.

5.3 Optimizing the mixing ratios for resistance response

Different mixing ratios of PEDOT-PSS/Carbon were investigated to reach an optimized value of the

electrical resistance response. Five different mixing ratios of 1, 2, 3, 4 and 5 wt% of PEDOT-PSS/Carbon pastes were tested and resistances were recorded for individual coating. The printing and curing conditions were kept the same for all the compositions and a two-probe test was conducted between the two opposite edges of the coated fiber. The resistance response for all the five compositions tested under same testing protocol are given in graph of Fig. 9. It is observed that the conductivity increases almost linearly by increasing the mixing ratio of PEDOT-PSS in synthesizing the nanocomposite mixture. A significant change in the base resistance, i.e., from 2.53 kΩ
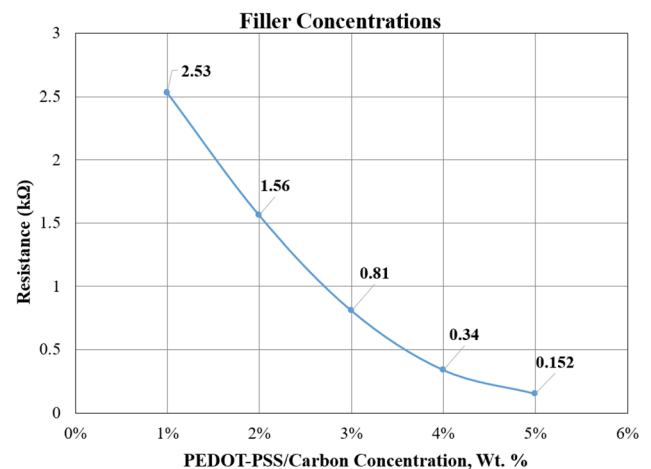
**Fig. 9** Resistance response for all the five compositions of PEDOT-PSS/Carbon paste tested under same testing protocol

to 152 Ω is recorded as we increase the mixing ratio from 1 to 5 wt%. This is good operating envelope of the sensor in general; however, certain important features need to be considered regarding the manufacturing and final pressure sensing-related applications. The ease in processing, i.e., casting or patterning the nanocomposite is the foremost priority, which allows uniform spreading of the ink as well as impregnating the fabric being absorbed completely within the threads. In this scenario, 2 wt% produced the best results in terms of printing and uniform coating of the desired sensing area. The resistance obtained with 2 wt% in the range of 1.5–1.6 kΩ is promising for the pressure-related sensing application. Graph in Fig. 9 shows the corresponding resistances obtained for each mixing composition. The operating window is large enough to respond to the corresponding pressures applied at top. Therefore, for all the experiments, 2 wt% of the nanocomposite is applied.

5.4 Sensor response to applied forces

To determine the pressure applied on each sensing block, commercially available force gauge (Mark 10) is used to apply force and simultaneously recording the change in resistance by using a digital multimeter. The percolation mechanism triggers the piezoresistance property in the impregnated fabric by generation of conducting channels. The initial base resistance is determined by the level of impregnation of the fabric threads and can be tuned by changing the nanocomposite compositions as shown in Fig. 9. For the testing purposes, only the 2 wt% concentration of the PEDOT-PSS/Carbon is selected based on their optimal properties such as uniform mixing of both the materials, better printability at controlled boundaries and finally producing reasonable operating windows for the resistance response. The sensors were tested at normal ambient conditions where the contacting wires were connected with each of the printed pads which is connected all the way to three sensors inline via printed interconnect lines. The two-part silver epoxy is used to make robust contacts at the pads that minimizes the contact resistance. The corresponding wires in the sensor array matrix are connected to the digital multimeter, while applying pressure individually at each corresponding sensor. For controlled force application, Mark 10 force gauge system is used, where the same size of contacting

surface as the sensor area is used to apply the uniform force at the sensor. The applied force is kept within a range of 1–5 N, at five different values as shown in Figure 10. Resistance at 0 N is about 1.650 kΩ and reduces all the way to about 115 Ω at 5 N, showing a significant change in the bulk resistance. Comparing to the results produced in [35, 36], the dynamic range of resistance response by sensor produced in this research is much higher. Besides the dynamic range, the response and restoration times are relative very high. The microscale deformation within the fabric threads as well as the intra-threads contact cause the resistance change. The range of forces detected with these sensors is suitable for a wide range of general purpose applications.

The sensors were evaluated for the cyclic force application to observe the restoration to the base resistance values after releasing the applied force. This helps in evaluating the existence of hysteresis particularly in the case of sandwiched sensory structures. For this case, the maximum load of 5 N is selected and applied for about 5 seconds and then releasing. Figure 11 shows the sensor response in this tapping mode by continuously applying force and releasing almost for the same interval of time. A rapid change (within the 30ms on average accounting for the steps) in the sensor response is observed. The restoration to baseline resistance is also very fast, taking almost similar time to the initial response. The pattern is similar, and it has been repeated for all the sensors, which repeated the same response and
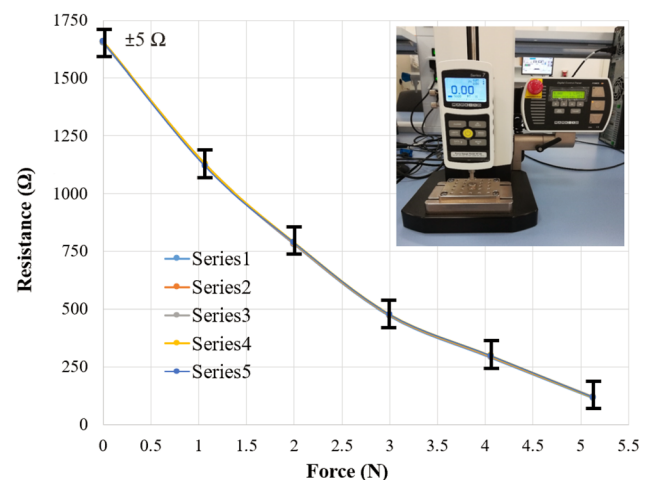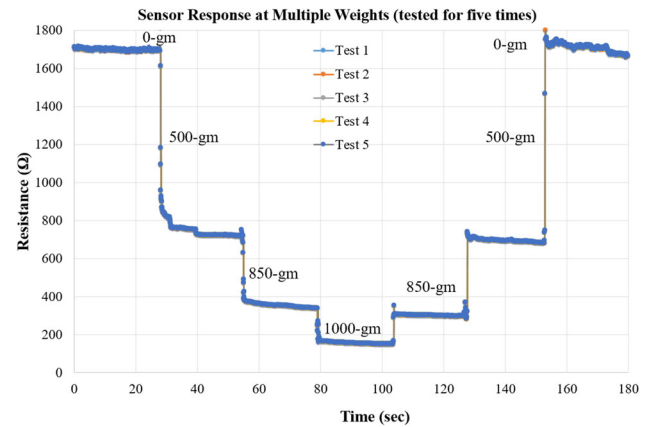

Fig. 10 Resistance response at applied force kept within a range of 1–5 N, at five varying steps (sensor tested for five different cycles)
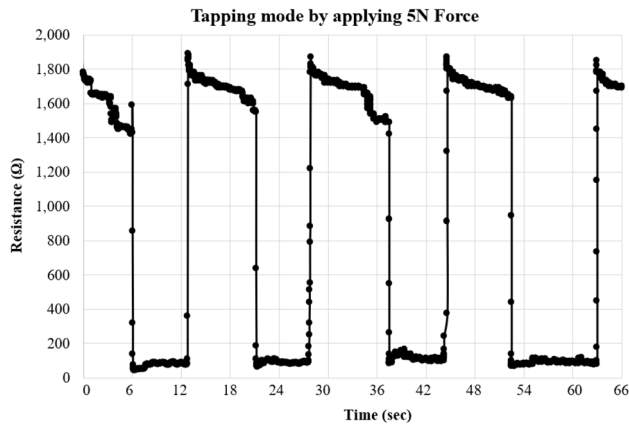
Fig. 11 Sensor response in tapping mode by continuously applying 5 N force and releasing almost for the same interval of time

Fig. 12 Results of the sensor response when different paper weights are placed consecutively on top of the sensory cells

restoration times. The change in base resistance is not abrupt, as the electrodes are not in intimate contact with the sensing layer. The instantaneous change corresponding to the applied force is observed only when both the electrodes make firm contact with the impregnated threads. This behavior is expected and was observed while testing all the sensing modules. The minor spikes occurring at the peaks are added by the contact resistance, but it suddenly lowers down as soon as an intimate contact is made. The sensors are left to normalize after each force cycle and takes about 10 seconds to reach the base resistance. This is because the conducting threads need the relaxation time to reach initial position. Reaching the baseline resistance after releasing the force seem to be higher; however, this change can be made as offset and compensated by the significant variation occurring only upon force application as well as after releasing.

For practical demonstration and real-time application, the sensor patch is used for monitoring of different weights in the form of trash paper. This research is focused on developing a type of sensor patch that could successfully be implemented for monitoring the fill level of trash especially discarded paper in a waste collection bin.Therefore, 3 different weights, i.e., 500 gm, 350 gm and 150 gm of the cellulose paper are placed on top of the sensor patch for such monitoring. The paper was cut in same size as the sensor patch area and was banded together. The sensor patch was placed on an elevated surface from the table-top, so as to be impacted only by the paper weight. Figure 12 shows results of the sensor response when paper weights are placed

consecutively on top of the sensory cells. Five set of tests were conducted an individual sensory cell to evaluate the repeatability of the sensor response. The instantaneous spikes are also observed here as well at the point of contacting the silver electrodes to the sensing layer. This however is insignificant when successive two weights are added to the first one. The sensing response to a minimum applied force as 1N as well as 150 gm weight is very promising detection limits, which are more suitable for developing a smart bin application. All the sensors were tested individually to examine the device variability and response variations as there is a probability of particles agglomeration at certain sites when nanocomposites are coated through screen-printing technology. This agglomeration might lead to a bulgy structure and would become the first contacting points with the electrodes even in the normal conditions. Therefore, the same testing setup and weights were used to monitor the device variability. Graph in Fig. 13 shows response of all the sensing devices tested under similar conditions and testing protocol. This test was repeated for ten times each to evaluate the precision of individual sensor. This however resulted in producing the same results with $\sim \pm 3$ ohms variability. The sensitivity graph is shown in Figure 14, which is evaluated from the data obtained for the resistance response of the sensor shown in Figure 12. It is evident from the graph in Fig. 13 that the devices are responsive in a close operating range with negligible variations. The slight variations are acceptable in response time as it is all the way translated from the initial base resistance. These could be minimized by allowing sufficient time for
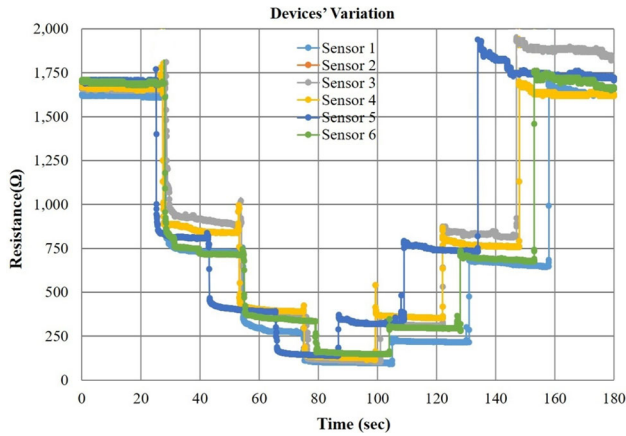
Fig. 13 Device variability tests by using the same testing setup and weights. Response of all the sensing devices tested under similar conditions and testing protocol
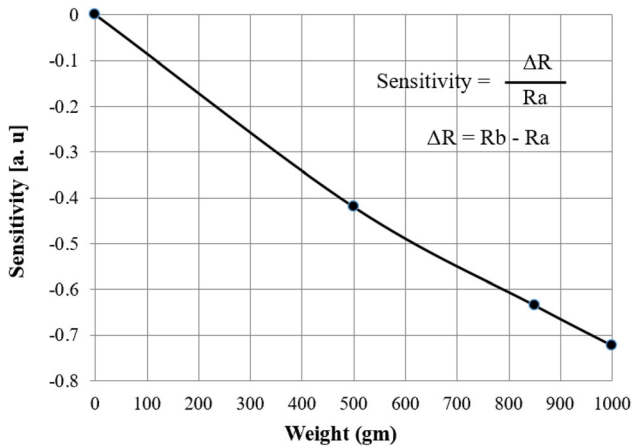
Fig. 14 Sensitivity of the sensor at corresponding weights

the sensing layer to relax and restore completely to the original position. The range of forces detected by these sensors lie in the normal range of forces (1–5N) experienced by human being in today life. Therefore, these types of sensors are ideal not only for smart paper bin fill level monitoring but also for many other exciting applications such pressure mapping of robotic skin, smart chairs for paralyzed persons and hospital beds. The prominent sensing parameters are compared with recently reported research as shown in Table 1 and it is observed that very promising results are obtained considering the sensitivity, response time as well as limit of detection. Although the results are not ideal but considering the large area manufacturing approach through an all-printing methodology make the process distinguished due to the simple and reduced fabrication steps. The less material wastage and efficient material deposition through printing make the process more cost-efficient. Considering the climatic conditions especially in the Middle East region, the sensor is tested in the range (25–52 °C) of temperatures, typically observed during the hot summer days. Slight variation in the resistances is observed as shown in the graph of Fig. 15, which need to be considered and filtered out using filter circuits in the signal processing board. Sensitivity of the sensor is evaluated against the corresponding weight forces.

6 Conclusion and future scope

This work presented an interesting development for making large area pressure sensor patch using cost-effective printing technologies. An investigative study is performed targeting the ease in processing, robust patterning, time, and material efficiency as well as the compatible integration of multiple layer and substrates. A stretchable fabric is made electrically conducting by impregnating it with a polymer-based nanocomposite solution. The sensory cells are developed by sandwiching the conductive fabric within two inkjet-printed Ag electrodes. A sensing array of 3×3 is developed having 5×5 mm^2 effective

Table 1 Comparison with previously reported nanocomposite-based pressure sensors

S. no	Sensing layer	Sensitivity	Response time	Limit of detection (g)	References
1	Carbon/Au	2×10^5/kPa	NA	2.55	[18]
2	Ag nanowires	1.5/kPa	3 s	3.0	[20]
3	Graphene oxides	0.72/kPa	$\sim$ 15ms	$\sim$ 10	[27]
4	Carbon cotton/PDMS	6.04/kPa	$\sim$ 1 s	2000	[34]
5	Carbon/PEDOT	1.45/kPa	$\sim$ 30 ms	150	This work
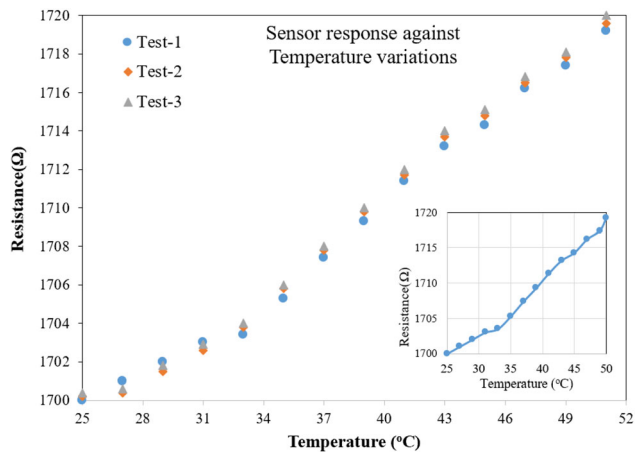
Fig. 15 Sensors response against temperature variations

sensing area. The nanocomposite is synthesized by mixing PEDOT-PSS and Carbon-based paste. Screen-printing technique is used to cast the synthesized solution at desired areas of the sensing device. Various evaluation techniques such as adhesion-loss test for detachment, optical and scanning electron microscopic analysis are performed. The sensors are tested in the range of 1-5 N using commercially available force gauge meter. A significant change in resistance of about 90% is observed by applying 5N force in a compressive manner that shows a wide range of application window for pressure sensing-related applications. Being targeted for applying in a paper trash bin, the sensors are also subjected practically by placing multiple weights in the form of paper trash. The sensor is observed to be responsive to as small as 150 gm of weight, which is an acceptable range for our application to monitor the level of weight in a paper trash bin. A full package of developing a wireless communication module is to be established as the future work to enable remote monitoring. Characterization of all sensing cells simultaneously and showing them as pressure maps in a graphical chart will be investigated to widen the application areas of this pressure sensing patch.

Acknowledgements

Declarations

Conflict of interest The authors declare that they have no conflict of interest.

References

1. Y. Khan, A. Thielens, S. Muin, J. Ting, C. Baumbauer, A.C. Arias, A new frontier of printed electronics: flexible hybrid electronics. Adv. Mater. **32**, 1905279 (2020)

2. S. Khan, L. Lorenzelli, R.S. Dahiya, Technologies for printing sensors and electronics over large flexible substrates: a review. IEEE Sens. J. **15**, 3164–3185 (2015)

3. J.C. Yeo, C.T. Lim, Emerging flexible and wearable physical sensing platforms for healthcare and biomedical applications. Microsyst. Nanoeng. **2**, 1–19 (2016)

4. A. Nag, S.C. Mukhopadhyay, J. Kosel, Wearable flexible sensors: a review. IEEE Sens. J. **17**, 3949–3960 (2017)

5. V. Beedasy, P.J. Smith, Printed electronics as prepared by inkjet printing. Materials **13**, 704 (2020)

6. F. Zheng, Z. Wang, J. Huang, Z. Li, Inkjet printing-based fabrication of microscale 3D ice structures. Microsyst. Nanoeng. **6**, 1–10 (2020)

7. N. Afsarimanesh, A. Nag, S. Sarkar, G.S. Sabet, T. Han, S.C. Mukhopadhyay, A review on fabrication, characterization and implementation of wearable strain sensors. Sens. Actuat. A **315**, 112355 (2020)

8. D. Maddipatla, B.B. Narakathu, M. Atashbar, Recent progress in manufacturing techniques of printed and flexible sensors: a review. Biosensors **10**, 199 (2020)

9. S. Khan, S. Ali, A. Bermak, Recent developments in printing flexible and wearable sensing electronics for healthcare applications. Sensors **19**, 1230 (2019)

10. L. Nayak, S. Mohanty, S.K. Nayak, A. Ramadoss, A review on inkjet printing of nanoparticle inks for flexible electronics. J. Mater. Chem. C **7**, 8771–8795 (2019)

11. W. Li, M. Vaseem, S. Yang, A. Shamim, Flexible and reconfigurable radio frequency electronics realized by high-throughput screen printing of vanadium dioxide switches. Microsyst. Nanoeng. **6**, 1–12 (2020)

12. C.G. Núñez, F. Liu, W.T. Navaraj, A. Christou, D. Shakthivel, R. Dahiya, Heterogeneous integration of contact-printed semiconductor nanowires for high-performance devices on large areas. Microsyst. Nanoeng. **4**, 1–15 (2018)

13. M. Singh, H.M. Haverinen, P. Dhagat, G.E. Jabbour, Inkjet printing—process and its applications. Adv. Mater **22**, 673–685 (2010)

14. J. Oliveira, V. Correia, H. Castro, P. Martins, S. Lanceros-Mendez, Polymer-based smart materials by printing technologies: Improving application and integration. Addit. Manuf. **21**, 269–283 (2018)

15. M. Gao, L. Li, Y. Song, Inkjet printing wearable electronic devices. J. Mater. Chem. C **5**, 2971–2993 (2017)

16. Y. Shu, C. Li, Z. Wang, W. Mi, Y. Li, T.-L. Ren, A Pressure sensing system for heart rate monitoring with polymer-based pressure sensors and an anti-interference post processing circuit. Sensors **15**, 3224–3235 (2015)

17. S. Ali, A. Hassan, S. Khan, A. Bermak, Flexible coplanar waveguide strain sensor based on printed silver nanocomposites. SN Appl. Sci. **1**, 744 (2019)

18. S.J.K. O'Neill, H. Gong, N. Matsuhisa, S. Chen, H. Moon, H.C. Wu et al., A carbon flower based flexible pressure sensor made from large-area coating. Adv. Mater. Interfaces **20**, 5 (2020). https://doi.org/10.1002/admi.202000875

19. S. Khan, W. Dang, L. Lorenzelli, R. Dahiya, Flexible pressure sensors based on screen printed P(VDF-TrFE) and P(VDF-TrFE)/MWCNTs. IEEE Trans. Semicond. Manufact. **28**, 486–493 (2015)

20. L. Gao, C. Zhu, L. Li, C. Zhang, J. Liu, H.-D. Yu et al., All paper-based flexible and wearable piezoresistive pressure sensor. ACS Appl. Mater. Interfaces. **11**, 25034–25042 (2019)

21. R. Dahiya, W.T. Navaraj, S. Khan, E.O. Polat, Developing electronic skin with the sense of touch. Frontline Technol. **31**, 6–10 (2015)

22. C.L. Popa, G. Carutasu, C.E. Cotet, N.L. Carutasu, T. Dobrescu, Smart city platform development for an automated waste collection system. Sustainability **9**, 2064 (2017)

23. J. Lee, H.-C. Kim, J.-W. Choi, I.H. Lee, A review on 3D printed smart devices for 4D printing. Int. J. Precis. Eng. Manufact.-Green Technol. **4**, 373–383 (2017)

24. H. Hwang, Y. Kim, J.H. Park, U. Jeong, 2D Percolation design with conductive microparticles for low-strain detection in a stretchable sensor. Adv. Func. Mater. **30**, 1908514 (2020)

25. M. Haghgoo, M. Hassanzadeh-Aghdam, R. Ansari, A comprehensive evaluation of piezoresistive response and percolation behavior of multiscale polymer-based nanocomposites. Compos. Part A **130**, 105735 (2020)

26. M.F. Clayton, R.A. Bilodeau, A.E. Bowden, D.T. Fullwood, Nanoparticle orientation distribution analysis and design for polymeric piezoresistive sensors. Sens. Actuat. A **303**, 111851 (2020)

27. M. Xu, F. Li, Z. Zhang, T. Shen, J. Qi, Piezoresistive sensors based on rGO 3D microarchitecture: coupled properties tuning in local/integral deformation. Adv. Electron. Mater. **5**, 1800461 (2019)

28. C.-W. Lai, S.-S. Yu, 3D printable strain sensors from deep eutectic solvents and cellulose nanocrystals. ACS Appl. Mater. Interfaces. **12**, 34235–34244 (2020)

29. R. Xie, Y. Xie, C.R. López-Barrón, K.-Z. Gao, N.J. Wagner, Ultra-stretchable conductive iono-elastomer and motion strain sensor system developed therefrom. Technol Innov **19**, 613–626 (2018)

30. Y.-Q. Li, P. Huang, W.-B. Zhu, S.-Y. Fu, N. Hu, K. Liao, Flexible wire-shaped strain sensor from cotton thread for human health and motion detection. Sci. Rep. **7**, 45013 (2017)

31. S. Khan, L. Lorenzelli, Recent advances of conductive nanocomposites in printed and flexible electronics. Smart Mater. Struct. **26**, 1083001 (2017)

32. H. Zhao, J. Bai, Highly sensitive piezo-resistive graphite nanoplatelet-carbon nanotubes hybrids/polydimethylsilicone composites with improved conductive network construction. ACS Appl. Mat. & Interfaces **7**, 9652–9659 (2015)

33. N. Yogeswaran, W. Dang, W.T. Navaraj, D. Shakthivel, S. Khan, E.O. Polat et al., New materials and advances in making electronic skin for interactive robots. Adv. Robot. **29**, 1359–1373 (2015)

34. Y. Li, Y.A. Samad, K. Liao, From cotton to wearable pressure sensor. J. Mater. Chem. A **3**, 2181–2187 (2015)

35. G. Kim, C.C. Vu, J. Kim, Single-layer pressure textile sensors with woven conductive yarn circuit. Appl. Sci. **10**, 2877 (2020)

36. S. Ali, S. Khan, A. Khan, A. Bermak, Developing conductive fabric threads for human respiratory rate monitoring. IEEE Sens. J. **21**, 4350–4356 (2020)